Initial Infarct Size Predicts Subsequent Cardiac Remodeling in the Rat Infarct Model: An In Vivo Serial Pinhole Gated SPECT Study

Fatiha Maskali, MSc[1,2]; Philippe R. Franken, MD[3]; Sylvain Poussier, PhD[2]; Nguyen Tran, PhD[4]; Chris Vanhove, PhD[3]; Henri Boutley, BSc[2]; Hervé Le Gall, MSc[5]; Gilles Karcher, MD[2]; Faïez Zannad, MD[1]; Patrick Lacolley, MD[1]; and Pierre Y. Marie, MD[1,2]

[1]UHP-INSERM U684, Faculty of Medicine, Nancy, France; [2]Nuclear Medicine Department, University Hospital, Nancy, France; [3]In Vivo Cellular and Molecular Imaging Center, University of Brussels (VUB), Brussels, Belgium; [4]Laboratory of Surgery School, Nancy, France; and [5]Superior National School of Chemical Industries, CNRS and INPL, Nancy, France

The rat infarct model is widely used to study left ventricular (LV) remodeling, a main cause of heart failure characterized by progressive LV dilatation. Using pinhole collimators and advances in data processing, gated SPECT was recently adapted to image the rat heart. The aim of this study was to assess this new imaging technique for predicting and quantifying variable LV remodeling from the rat infarct model. **Methods:** Pinhole ^{99m}Tc-sestamibi gated SPECT was validated for determining LV volume and identifying the necrotic and nonviable LV segments (<50% of ^{99m}Tc-sestamibi uptake) in rats, and it was applied to monitor rat LV function from 48 h to 12 wk after occlusion of the left anterior descending coronary artery (LAD) (n = 20) or sham operation (n = 9). **Results:** In LAD-occluded rats, 48-h SPECT necrosis was large (≥30% LV) in 6, limited (<30% LV) in 6, and undetectable in 8. End-diastolic volume of LAD-occluded rats was equivalent to that of sham-operated rats at 48 h (320 ± 84 μL vs. 293 ± 48 μL; not significant) but became higher at 12 wk (501 ± 191 μL vs. 343 ± 46 μL; P = 0.01). The follow-up increase in end-diastolic volume, which reflects the remodeling process, was closely related to the initial extent of necrosis revealed by the SPECT images ($P < 0.001$; R^2 = 0.85). This increase was limited in sham-operated rats (50 ± 15 μL) and in the LAD-occluded rats with undetectable necrosis (55 ± 35 μL) but it was around 3- and 7-fold higher in the LAD-occluded rats with limited (165 ± 57 μL) and large (366 ± 113 μL) necrosis, respectively. **Conclusion:** The variable LV remodeling documented after coronary occlusion in rats closely relates to the variable extent of necrosis provided by this model. Pinhole gated SPECT allows this remodeling to be predicted and quantified and, hence, constitutes an original tool for the experiments scheduled on the rat infarct model.

Key Words: remodeling; myocardial infarction; rat; gated SPECT; sestamibi

J Nucl Med 2006; 47:337–344

Left ventricular (LV) remodeling is defined by progressive dilatation and altered geometry and is a main cause of heart failure in humans (*1*). Because of its accurate reflection of human pathophysiology (*2*), the rat infarct model has been widely used to study LV remodeling after myocardial infarction. Such studies are warranted when novel strategies are planned to limit infarct size or to retard progression toward heart failure. Unfortunately, because of variability in coronary anatomy and collateral circulation, coronary occlusion produces variable areas of necrosis in rats (*2–8*). In addition, postmortem histopathologic analyses have shown that the extent of necrosis was a main determinant of LV remodeling in this model (*2–4,7,8*). Consequently, variable LV remodeling is provided by the rat infarct model. This constitutes a strong limitation when assessing therapeutic interventions and, thus, a technique allowing this remodeling to be predicted would be helpful.

In humans, ^{99m}Tc-sestamibi SPECT is currently used in the setting of ischemic LV remodeling and it has been extensively validated for (i) differentiating viable from predominantly necrotic myocardium using the threshold value of 50% uptake (*9–13*), (ii) sizing myocardial infarction (*14–16*), (iii) predicting the evolution of LV function after infarction (*9,10,17*), and (iv) determining LV function on gated SPECT acquisitions (*18*). Thanks to the use of pinhole collimators and to advances in data processing, gated SPECT was recently adapted to image the rat heart (*19*). The present study was aimed to assess this new imaging technique for predicting and quantifying variable LV remodeling from the rat infarct model.

MATERIALS AND METHODS

Twenty-nine adult male Wistar rats (Charles Rivers Laboratories; 13- to 15-wk old; 460- to 540-g body weight at the beginning of the study) were enrolled. This study was conducted according to the recommendations of our local ethical committee and to the National Institutes of Health principles of laboratory animal care

Received Sep. 2, 2005; revision accepted Nov. 7, 2005.

For correspondence contact: Fatiha Maskali, MSc. Unité mixte INSERM-UHP U684, Faculté de Médecine de Nancy, 54505 Vandoeuvre-Les-Nancy, France.

E-mail: fatiha.maskali@medecine.uhp-nancy.fr

(NIH publication 86-23, revised 1985). The animals were submitted either to sham operation ($n = 9$) or to surgical coronary occlusion ($n = 20$) and they were subsequently monitored in vivo by serial ^{99m}Tc-sestamibi pinhole gated SPECT performed at 48 h and at 2, 6, and 12 wk after surgery. To provide validation of the image data, 15 rats were sacrificed and the repartitions of myocardial fibrosis, cellular loss, and ^{99m}Tc-sestamibi activity were determined on histologic sections.

Additional experiments were conducted on cardiac rat phantoms of various sizes to assess the accuracy of LV volumes measured with pinhole gated SPECT.

Surgical Procedure

Permanent coronary occlusion of the left anterior descending coronary artery (LAD) was performed according to the usual and extensively described method (*2–8*). The rats were anesthetized by inhalation of an isoflurane/oxygen mixture and administration of ketamine hydrochloride (10 mg/kg). They were intubated and artificially ventilated with a rodent ventilator (Harvard Apparatus). The heart was exposed through a left lateral thoracotomy of the fifth interrib space. After pericardial incision, the proximal part of the LAD was ligated with a 7-0 Prolene suture (Ethicon, Inc.), at 2–3 mm from the left atrium tip. Finally, the chest was closed in layers with a 2-0 Vicryl suture (Ethicon, Inc.), the lungs were reinflated using positive-end expiratory pressure, and the endotracheal tube was removed once spontaneous breathing had resumed. Sham-operated rats had exactly the same surgical procedure, except that the LAD was not ligated.

Serial Pinhole Gated SPECT Acquisitions

The animals were sedated by intraperitoneal injection of 60 mg/kg of sodium pentobarbital, and ^{99m}Tc-sestamibi (400–700 MBq in a 0.3- to 0.5-mL volume) was injected intravenously 40–60 min before starting gated SPECT acquisition. During the acquisition, the animals were in prone position and were connected to a standard electrocardiogram monitor by 3 electrodes placed on the inner surfaces of limb extremities.

As previously described (*19*), pinhole gated SPECT acquisitions were performed using a conventional single-head γ-camera (DSX; General Electric-SMV) equipped with a 3-mm pinhole collimator (195-mm focal length; 43-mm radius of rotation). Thirty-two projections of 30 s each were acquired on a 180° anterior circular orbit centered on the heart (from 110° right-anterior to 290° left-anterior orientations). The use of 180° instead of 360° orbit allowed the rotation radius of the camera head to be reduced and, thereby, the spatial resolution of pinhole SPECT images was further enhanced. Additional acquisition parameters were as follows: 64×64 matrix, 2.66 zoom, 16 bins, 126- to 154-keV energy window, beat acceptance window set to ±20% of averaged R–R interval. Total acquisition time was 16 min.

Reconstruction and Analysis of Pinhole Gated SPECT Images

As already described (*19–21*), projection data were corrected for the mechanical shift of the camera-head rotation and for the nonuniform sensitivity of pinhole detection. Images were thereafter reconstructed using an ordered-subset expectation maximization (OSEM) iterative process (2 iterations and 8 subsets), which was adapted, first, to take into account pinhole geometry and, second, to reduce noise by incorporating a temporal Fourier filtering after each iteration (*19–21*). Voxel size of the reconstructed images was 0.6 mm and the spatial resolution was 3 mm in the central slice when determined by the full width at half maximum on a point source of ^{99m}Tc.

Cardiac reorientation along the LV long axis was performed using standard clinical software (Mirage Processing Application; Segami). LV end-diastolic volume (EDV) and end-systolic volume (ESV), as well as LV ejection fraction (EF), were determined by QGS software (*22,23*) on contiguous gated short-axis slices. Sestamibi uptake was determined on the set of collapsed short-axis slices with QPS software (*23*) and the 17-segment LV division from the American Heart Association (*24*). The 2 proximal septal segments, corresponding to the membranous part of the septal wall, were excluded. For both QGS and QPS, constraint limits of contour detection were applied only in case of evident errors with the fully automatic process.

Phantom Study

To assess the accuracy of LV volumes measured with pinhole SPECT, the protocols of data acquisition, reconstruction, and quantitative analyses were applied to LV rat phantoms of various volumes ranging from 50 to 800 μL. These phantoms were obtained by a stereolithography process, which allows fabricating small objects of any shape with a 0.1-mm precision and by using 3-dimensional computer-aided design (*25*).

As illustrated in Figure 1, these phantoms were comprised of an internal cavity filled with water and an external wall cavity with a thickness of 2.1 mm, corresponding to that of rat LV walls in vivo (*26,27*). The wall cavity was filled with a solution containing 0.14 MBq of ^{99m}Tc per microliter.

Histologic Section Analyses

Histologic sections were analyzed to further characterize the segments showing <50% sestamibi uptake in vivo on pinhole SPECT: determinations of their sestamibi activity in vitro as well as their percentages of volume fibrosis and of cellular loss.

For this purpose, rats were sacrificed with an overdose of sodium pentobarbital, 50 min after the intravenous injection of 180 MBq of ^{99m}Tc-sestamibi and 2–5 d after the last 12-wk pinhole SPECT. The hearts were excised, arrested in ice-cold potassium chloride (2 mol/L), and snap frozen in liquid nitrogen. Contiguous sections (8–10 μm), orientated along the vertical or horizontal long axis of the LV (depending on infarct location), were obtained in a cryostat at 22°C. One midventricular section was selected and immediately referred to a 48-h recording with a μIMAGER (Biospace) (*28,29*) for quantifying the distribution of ^{99m}Tc-sestamibi activity (voxel size, 20 μm). This section was thereafter stained by collagen-specific Sirius red and analyzed using light microscopy and a dedicated computer analysis system to measure the wall thickness and percentage of volume fibrosis (*30*).

Histologic sections, as well as their corresponding 12-wk pinhole SPECT slices, were divided into the same 7 segments, which were those visualized on long-axis slices according to the 17-segment LV division from the American Heart Association (*24*). Segments with <50% uptake on pinhole SPECT were identified in each section and compared with the remote segments, which were those not directly adjacent. ^{99m}Tc-Sestamibi activity was determined on μIMAGER images using hand-drawn regions of interests encompassing each segment. In segments associated with <50% uptake on pinhole SPECT, this activity was expressed by mean voxel values and in the percentage of average values from remote segments. Volume fibrosis percentage was calculated in each segment on the Sirius red–stained sections by averaging values from 4 to 6 sampling areas of

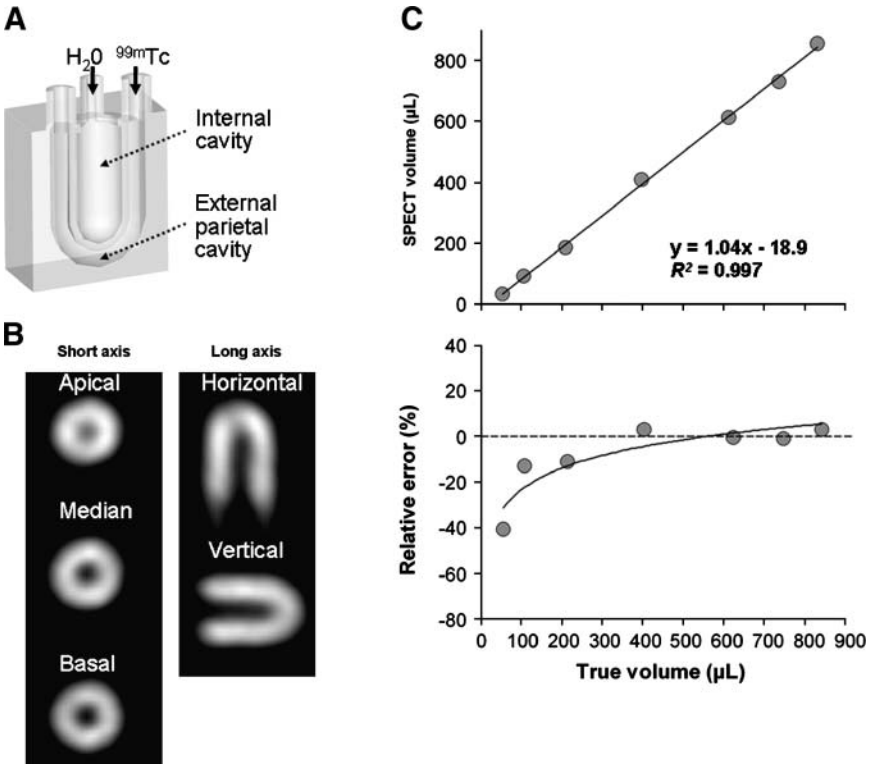

FIGURE 1. Rat cardiac phantom experiments. (A) Schematic representation of phantoms. (B) Example of pinhole SPECT images obtained on 200-μL phantom. (C) Relationships between real values of phantom volumes and either phantom volumes determined by pinhole SPECT (top) or relative error in the volume determination provided by pinhole SPECT (bottom).

0.1–0.3 mm^2 each. The wall thickness of each segment was averaged from 3 to 6 measurements. The product of wall thickness by the fraction of nonfibrotic tissue was used as an index of viable tissue (*31*) and percentages of cellular loss were determined in segments with <50% uptake using the formula: $(V_2 - V_1)/V_2 \times 100$, where V_1 is the index of viable tissue of the considered segment and V_2 is the mean value of indices determined in remote segments from the same slice (*31*).

Statistical Analysis

Quantitative variables were expressed as mean ± SD and compared with nonparametric tests: the Wilcoxon rank sum test was used for paired series and the Kurskal–Wallis test was used for multigroup unpaired comparisons. A P value < 0.05 was considered to be significant. Multivariate analyses were performed stepwise using ascending linear regression analyses (SPSS 10.0 statistical software). At each step, the limits for significance to enter and remove a variable were 0.05 and 0.10, respectively.

RESULTS

Validation of Volume Measurement

Results from the phantom study are displayed in Figure 1. There was a close relationship between real volumes of phantom cavities and those determined on SPECT images ($R^2 = 0.997$), and a significant imprecision was only documented for the smallest 50-μL phantom (40% volume underestimation).

Characterization of Segments with <50% Sestamibi Uptake

Among the 105 segments analyzed on the histologic sections, 27 showed <50% of sestamibi uptake on the pinhole SPECT performed before sacrifice. The decrease in ^{99m}Tc-sestamibi activity, which was calculated in each of these 27 segments with regard to remote slice segments, was equivalent when determined in vitro on μIMAGER sections (−54% ± 22%) and in vivo on the corresponding SPECT slices (−56% ± 18%). Moreover, these 27 segments had a much higher volume fibrosis (in % of myocardial volume: 27% ± 20% vs. 5% ± 7%; $P < 0.001$) and a much lower parietal thickness (2.0 ± 1.5 mm vs. 3.9 ± 1.0 mm; $P < 0.001$) than remote slice segments. Finally, segments with <50% uptake on pinhole SPECT had an estimated 61% ± 33% cellular loss compared with remote segments, with >50% cellular loss being observed in 74% of these segments (20/27). Pinhole SPECT identification of necrotic myocardium is illustrated in Figure 2 by SPECT, μIMAGER, and histologic images obtained in the same animals.

Quantitative Measurements at 48 Hours After Surgery

The mean body weight of the 20 rats with LAD occlusion (492 ± 30 g) was equivalent to that of the 9 sham-operated rats (492 ± 36 g).

Predominantly necrotic segments, defined as those with <50% sestamibi uptake on pinhole SPECT (nonviable myocardium), were observed in 12 of the 20 LAD-occluded rats (60%): 6 had a large necrotic area involving at least 5 segments (≥30% of LV) and the 6 others had a more limited necrotic area, involving <5 LV segments (<30% of LV). No segment with <50% sestamibi uptake was documented on the SPECT images from the remaining 8 LAD-occluded rats and from the 9 sham-operated rats.

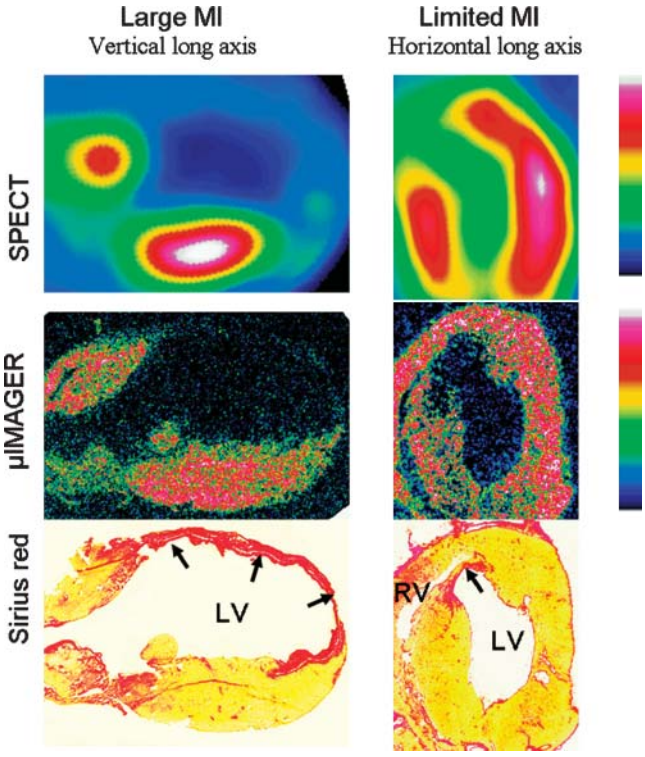

FIGURE 2. Images recorded in 2 rats exhibiting either large myocardial infarction (Large MI, left) or small myocardial infarction (Limited MI, right): long-axis slices from ^{99m}Tc-sestamibi pinhole SPECT (top) and corresponding histologic sections with μIMAGER recording of ^{99m}Tc-sestamibi activity (middle) and red Sirius staining (bottom). Necrotic walls (black arrows) are characterized by thinning and enhanced fibrosis (red coloration by red Sirius) and by marked decrease in sestamibi uptake on both μIMAGER and SPECT images. Areas with <50% uptake on pinhole SPECT exceed slightly those with real necrosis (apical part of inferior wall on left; apical part of septal wall on right), giving evidence of a trend toward necrosis overestimation. LV = left ventricle; RV = right ventricle.

EDV of LAD-occluded rats was equivalent to that of sham-operated rats at 48 h (320 ± 84 μL vs. 293 ± 48 μL; not significant). In addition, these 2 groups did not differ in ESV and EF at 48 h (Table 1). On subgroup analyses, however, significant differences were documented between the sham-operated rats and the LAD-occluded rats with large necrosis (≥30% of LV) for ESV, EDV, and EF (Fig. 3).

Follow-up by Serial Pinhole Gated SPECT

During the 12-wk follow-up, LAD-occluded rats exhibited a significant though limited increase in SPECT infarct size (from 14% ± 14% of LV to 16% ± 16% of LV; $P = 0.03$) and, on subgroup analyses, a trend toward an increase in infarct size was documented for rats with large necrosis at 48 h (≥30% of LV; $P = 0.08$) and, to a lesser extent, for those with small necrosis (<30% of LV; $P = 0.18$). LAD-occluded rats had, moreover, marked increases in EDV and ESV, whereas sham-operated rats had only slight volume variations during the same period (Table 1). Consequently, EDV of LAD-occluded rats became clearly higher than that of sham-operated rats at 12 weeks (501 ± 191 μL vs. 343 ± 46 μL; $P = 0.01$) (Table 1).

As illustrated in Figure 3, the increase in EDV during follow-up, which reflects the remodeling process, was limited in sham-operated rats (50 ± 15 μL) and in the LAD-occluded rats with undetectable SPECT necrosis (55 ± 35 μL), but it was around 3- and 7-fold higher in the LAD-occluded rats with limited (165 ± 57 μL) and large (366 ± 113 μL) SPECT necrosis, respectively. In addition, only the LAD-occluded rats showing a large necrosis (≥30% of LV) had a persistent increase in EDV during the second half of follow-up (between 6- and 12-wk values). At 12 wk, finally, LV function became (i) severely affected in the LAD-occluded rats with large SPECT necrosis (EF, 29% ± 7%; EDV, 742 ± 136 μL; all $P < 0.05$ vs. all other groups), (ii) much less affected in those with more limited SPECT necrosis (EF, 47% ± 6%; EDV, 472 ± 84 μL; all $P < 0.05$ vs. all other groups), and (iii) preserved in the LAD-occluded rats with undetectable SPECT necrosis (EF, 57% ± 8%; EDV, 342 ± 40 μL), as well as in sham-operated rats (EF, 55% ± 5%; EDV, 342 ± 46 μL). These data are illustrated by the SPECT images displayed in Figure 4.

On multivariate analyses, involving all 48-h SPECT data (extent of SPECT necrosis, EF, EDV, and ESV), as well as age and body weight of rats at 48 h, the best independent predictor of follow-up variations in EDV was the SPECT infarct size determined at 48 h ($P < 0.001$). When this parameter was excluded, the best independent predictor became the 48-h EF ($P < 0.001$). The extent of 48-h SPECT infarction allowed prediction of 85% of follow-up variations in EDV, whereas the corresponding percentage was only 44% for the prediction provided by 48-h EF. Relationships between the changes in LV volume during follow-up and the initial 48-h values of either infarct size or EF are detailed in Figure 5.

DISCUSSION

In the present study, ^{99m}Tc-sestamibi gated SPECT was successfully applied to the rat infarction model, thanks to the use of pinhole collimators and to recent advances in data processing (4-dimensional OSEM filtering (*19*)). This noninvasive technique provides a determination of LV function, as well as an identification of the necrotic nonviable LV segments, as those obtained routinely by rest gated SPECT in coronary artery disease (CAD) patients (*9–18*).

Pinhole ungated SPECT has already been applied in the rat infarct model (*32,33*) and our pinhole gated SPECT technique was previously shown to provide precise and reproducible determinations of LV volume and EF in normal adult rats (*19*). By using cardiac phantoms, we documented here the accuracy of volume measurement over a much larger range of values: from 100 μL, corresponding to ESV of normal adult rats, up to >800 μL, corresponding to the largest EDVs after infarction in rats (*3,4,19,26*).

TABLE 1
Comparisons Between Rats with LAD Occlusion and Those with Sham Operation: Pinhole SPECT Data at 48 Hours and at 12 Weeks After Surgery and Absolute Variations of These Data between 48 Hours and 12 Weeks

Parameter	LAD occlusion (n = 20)	Sham operation (n = 9)	P value
48-h pinhole SPECT			
Necrotic myocardium (% LV)	14 ± 14	0 ± 0	0.004
End-diastolic volume (μL)	320 ± 84	293 ± 48	NS
End-systolic volume (μL)	146 ± 71	113 ± 10	NS
Ejection fraction (%)	56 ± 12	61 ± 4	NS
12-wk pinhole SPECT			
Necrotic myocardium (% LV)	16 ± 16	0 ± 0	0.004
End-diastolic volume (μL)	501 ± 191	343 ± 46	0.01
End-systolic volume (μL)	294 ± 183	154 ± 24	0.03
Ejection fraction (%)	46 ± 13	55 ± 5	0.05
Absolute variations between 48 h and 12 wk			
Necrotic myocardium (% LV)	2 ± 3	0 ± 0	NS
End-diastolic volume (μL)	182 ± 149	50 ± 15	0.002
End-systolic volume (μL)	148 ± 133	40 ± 17	0.01
Ejection fraction (%)	−10 ± 9	−5 ± 6	NS

LAD = left anterior descending coronary artery; LV = left ventricle; NS = nonsignificant.

In CAD patients, predominantly necrotic myocardium is routinely characterized by ^{99m}Tc-sestamibi uptake being <50% of the maximal LV value on rest SPECT acquisition. This corresponds to histologic evidence of chronically infarcted myocardium (extended fibrosis, cellular loss) and to a very low potential for further functional recovery (*9–13*). The present study gives evidence, first, that the segments with <50% uptake on pinhole SPECT truly had a dramatic decrease in ^{99m}Tc-sestamibi activity. Indeed, on average, these segments had a >50% decrease in the tracer activity when determined in vitro, after animal sacrifice, and with regard to remote segments from the same histologic slices. Second, these segments with <50% uptake on pinhole SPECT had characteristics similar to those documented in CAD patients for the predominantly necrotic myocardial segments termed nonviable (*13,31,34*): nearly 30% volume fibrosis and >50% cellular loss, on average. Among segments with <50% uptake, however, 26% did not show >50% cellular loss, a reliable criterion of nonviable myocardium (*31*). This provides evidence that nonviable myocardium is slightly overestimated by this criterion, as illustrated by the SPECT images displayed in Figure 4, and the role of the

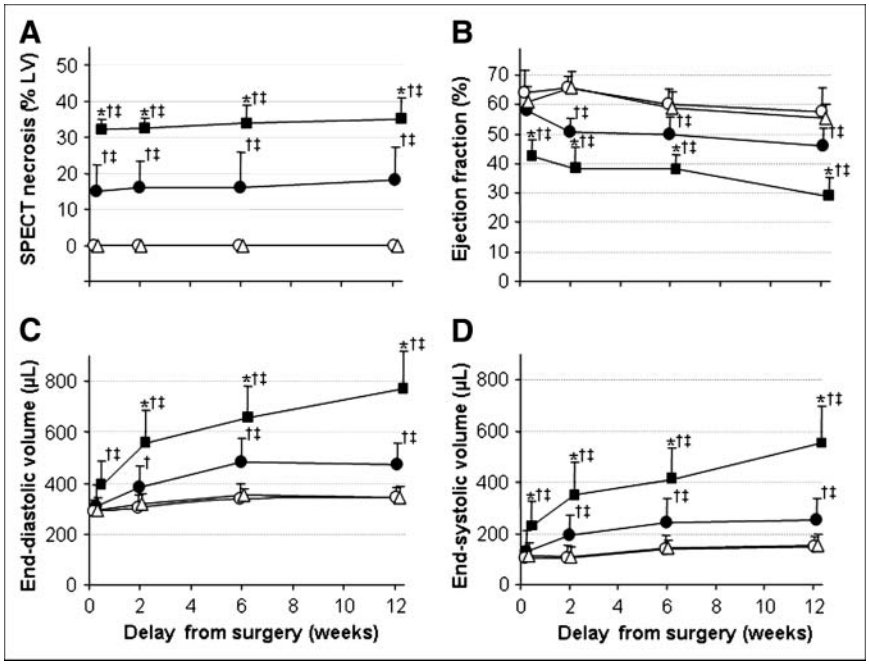

FIGURE 3. Comparisons between sham-operated rats (△; n = 9) and rats with LAD occlusion and large (≥30% of LV; ■; n = 6), limited (<30% of LV; ●; n = 6), or undetectable (○; n = 8) 48-h SPECT necrosis. (A) SPECT necrosis. (B) EF. (C) EDV. (D) ESV. *P < 0.05 for comparisons vs. rats with limited necrosis (<30% LV). †P < 0.05 for comparisons vs. rats with undetectable necrosis. ‡P < 0.05 for comparisons vs. sham-operated rats.

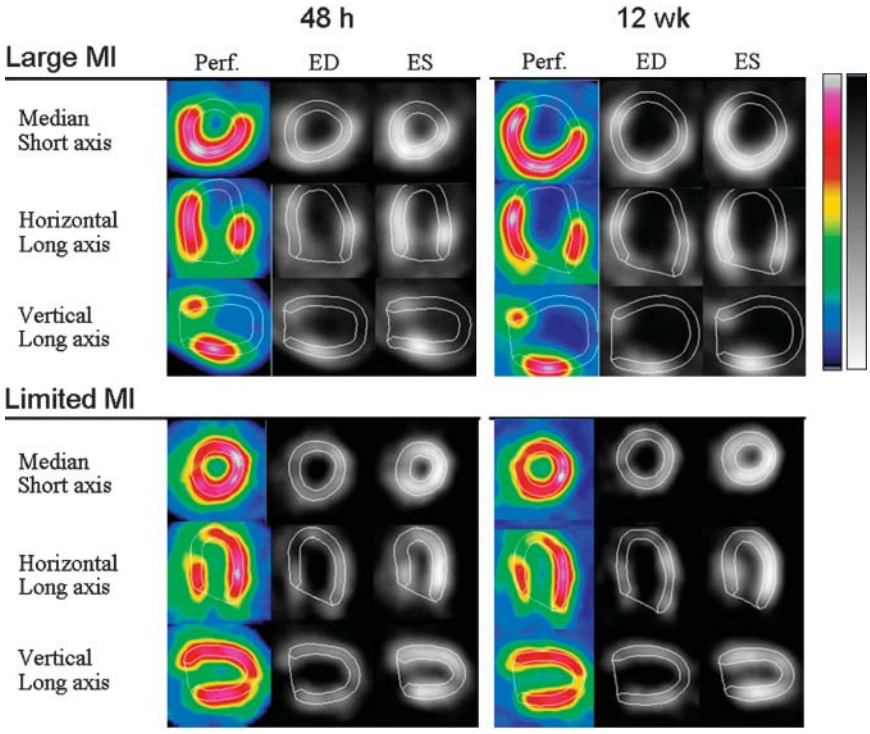

FIGURE 4. Images from perfusion SPECT (Perf.) and from end-systolic (ES) and end-diastolic (ED) gated SPECT, which were recorded at 48 h (left) and at 12 wk (right) after myocardial infarction (MI) in the 2 rats presented in Figure 2. In the rat with large MI (top), LV remodeling was dramatic between 48 h (EF, 49%; EDV, 407 μL) and 12 wk (EF, 30%; EDV, 850 μL). In the rat with limited MI (bottom), LV remodeling was much lower between 48 h (EF, 57%; EDV, 330 μL) and 12 wk (EF, 52%; EDV: 385 μL).

partial-volume effect might be questioned. This necrosis overestimation was, however, already documented for conventional sestamibi SPECT in CAD patients (*11–13*), and recent reports have shown that it might be prevented while injecting sestamibi after nitrate administration (*35*). The value of this method, which enhances sestamibi uptake within viable but severely ischemic myocardium, remains to be addressed on the rat infarct model.

In the present study, predominantly necrotic LV segments, as defined by <50% of sestamibi uptake, were detected in vivo by pinhole SPECT as early as 48 h after LAD occlusion in adult rats. Using this criterion, significant necrosis was absent in as many as 40% of cases, limited (<30% LV) in 30%, and large (≥30% LV) in 30%. Similar proportions were previously documented by histologic postmortem analyses (*2–4,7,8*). Because of variability in coronary anatomy and

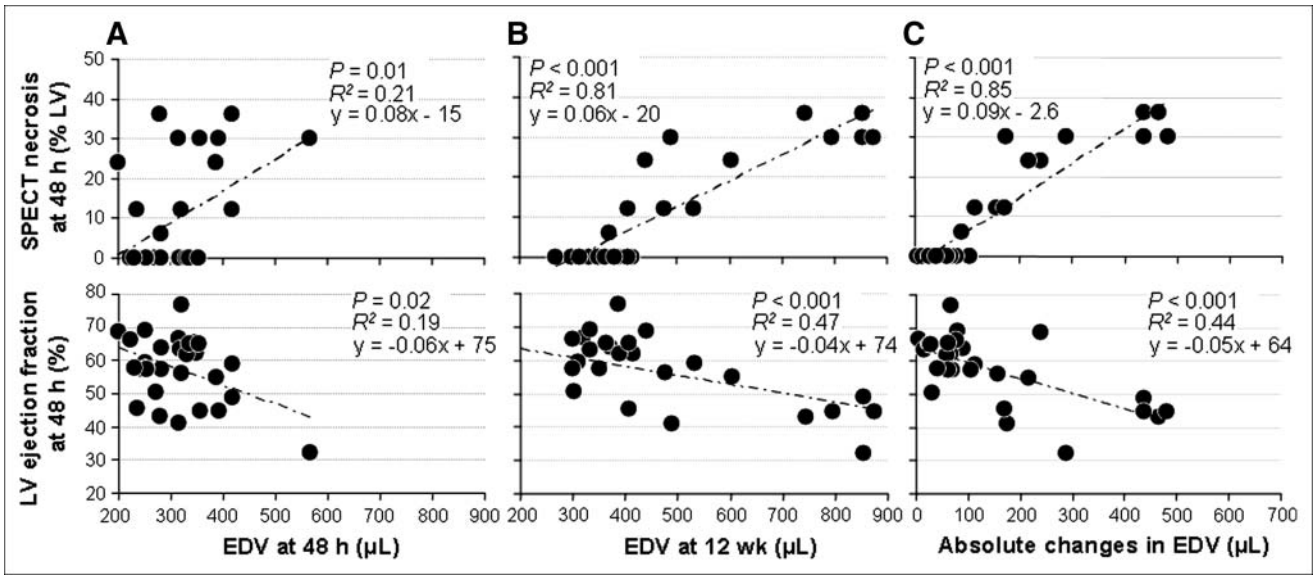

FIGURE 5. Relationships between initial values of either SPECT infarct size (top) or EF (bottom) determined 48 h after surgery and EDVs determined at 48 h (A) and 12 wk (B) and absolute changes in EDV between 48 h and 12 wk (C). Initial 48-h values of both EF and infarct size are poorly related to 48-h EDV but strongly related to 12-wk EDV and to absolute changes in EDV. However, these relationships are much closer with 48-h infarct size than with 48-h EF.

collateral circulation, coronary occlusion is known to provide variable areas of infarction in rats (*2–8*).

During subsequent follow-up, there was a significant though limited enlargement of the SPECT infarct size, especially when a large infarct area (≥30% LV) was documented at 48 h. This observation is likely to relate to the thinning and expansion of necrotic areas. Indeed, both have been consistently documented by previous histologic studies of transmural infarction in rat (*2,3*) and they might be the result of myocyte slippage (a decrease in the number of cells across the wall) (*36*). Moreover, LV remodeling was closely related to SPECT infarct size determined at 48 h: the increase in EDV was high and sustained during the overall 12-wk follow-up in rats with large infarction, much lower and limited to the first half of follow-up in rats with smaller infarction, and, finally, rats with undetectable SPECT necrosis evolved similarly to sham-operated ones. As much as 85% of the further increase in EDV could be predicted by initial infarct size. This provides evidence that the variable LV remodeling, documented after LAD occlusion in adult male Wistar rats, is primarily related to the variable extent of the necrotic area. This situation is, therefore, different from that of CAD patients, in whom ischemic remodeling might be more variable according to inherited characteristics and to acquired diseases (diabetes, hypertension, aging, etc.) (*1*).

In a previous echographic study of the rat infarct model, an early decrease in LV function (LV fractional shortening) was found to be a good predictor of further remodeling (*7*). Similar results were achieved in the present study with the LV EF determined at 48 h. The extent of SPECT necrosis was, however, a much better predictor, as evidenced by results displayed in Figure 5. Other studies had already shown that the amount and duration of LV remodeling were related to infarct size (*2–4,7,8*) but this size was determined by postmortem histologic analyses and, thus, it could not be used to predict further remodeling. The dual noninvasive determinations of infarct size and LV function, which are provided by pinhole gated SPECT, might be particularly useful when assessing therapeutic interventions on the rat infarct model. It is likely that such interventions may have very different effects according to the initial infarct size and, thus, to the expected further remodeling.

CONCLUSION

This study shows that the variable LV remodeling, which is documented after coronary occlusion in rats, closely relates to the variable infarct size provided by this model. Pinhole gated SPECT allows this remodeling to be predicted and quantified and, hence, constitutes an original tool for the experiments scheduled on the rat infarct model.

ACKNOWLEDGMENTS

The authors thank the Association for Research and Scientific Information in Cardiology, the Lorraine Region, and the Foundation of France for Research on Cardiovascular Diseases for financial support; the University Hospital from Nancy for organizational support; Jean-Marc Gravier for his help in data processing; the staff of SMV-General Electric France, especially Dominique Marlier, for technical support; and Jean-Marc Virion for his help in statistical analyses.

REFERENCES

1. Cohn JN, Ferrari R, Sharpe N. Cardiac remodeling: concepts and clinical implications—a consensus paper from an international forum on cardiac remodeling. *J Am Coll Cardiol.* 2000;35:569–582.
2. Goldman S, Raya TE. Rat infarct model of myocardial infarction and heart failure. *J Card Fail.* 1995;1:169–177.
3. Pfeffer JM, Pfeffer MA, Fletcher PJ, et al. Progressive ventricular remodeling in rat with myocardial infarction. *Am J Physiol.* 1991;260:H1406–H1414.
4. Pfeffer JM, Pfeffer MA, Fletcher PJ, et al. Ventricular performance in rats with myocardial infarction and failure. *Am J Med.* 1984;76:99–103.
5. Spadaro J, Fishbein MC, Hare C, et al. Characterization of myocardial infarcts in the rat. *Arch Pathol Lab Med.* 1980;104:179–183.
6. Ye J, Yang L, Sethi R, et al. A new technique of coronary artery ligation: experimental myocardial infarction in rats in vivo with reduced mortality. *Mol Cell Biochem.* 1997;176:227–233.
7. Solomon SD, Greaves SC, Rayan M, et al. Temporal dissociation of left ventricular function and remodeling following experimental myocardial infarction in rats. *J Card Fail.* 1999;5:213–223.
8. Weisman HF, Bush DE, Mannisi JA, et al. Global cardiac remodeling after acute myocardial infarction: a study in the rat model. *J Am Coll Cardiol.* 1985;5: 1355–1362.
9. Bax JJ, van der Wall EE, Harbinson M. Radionuclide techniques for the assessment of myocardial viability and hibernation. *Heart.* 2004;90:v26–v33.
10. Underwood SR, Bax JJ, vom Dahl J, et al. Study Group of the European Society of Cardiology: imaging techniques for the assessment of myocardial hibernation—report of a Study Group of the European Society of Cardiology. *Eur Heart J.* 2004;25:815–836.
11. Maes AF, Borgers M, Flameng W, et al. Assessment of myocardial viability in chronic coronary artery disease using technetium-99m sestamibi SPECT; correlation with histologic and positron emission tomographic studies and functional follow-up. *J Am Coll Cardiol.* 1997;29:62–68.
12. Medrano R, Lowry RW, Young JB, et al. Assessment of myocardial viability with ^{99m}Tc sestamibi in patients undergoing cardiac transplantation: a scintigraphic/pathological study. *Circulation.* 1996;94:1010–1017.
13. Dakik HA, Howell JF, Lawrie GM, et al. Assessment of myocardial viability with ^{99m}Tc-sestamibi tomography before coronary bypass graft surgery: correlation with histopathology and postoperative improvement in cardiac function. *Circulation.* 1997;96:2892–2898.
14. Miller TD, Christian TF, Hopfenspirger MR, et al. Infarct size after acute myocardial infarction measured by quantitative tomographic ^{99m}Tc sestamibi imaging predicts subsequent mortality. *Circulation.* 1995;92:334–341.
15. Gibbons RJ, Miller TD, Christian TF. Infarct size measured by single photon emission computed tomographic imaging with ^{99m}Tc-sestamibi: a measure of the efficacy of therapy in acute myocardial infarction. *Circulation.* 2000;101: 101–108.
16. van der Wall EE, Niemeyer MG, de Roos A, et al. Infarct sizing by scintigraphic techniques and nuclear magnetic resonance imaging. *Eur J Nucl Med.* 1990;17: 83–90.
17. Lipiecki J, Cachin F, Durel N, et al. Influence of infarct-zone viability detected by rest Tc-99m sestamibi gated SPECT on left ventricular remodeling after acute myocardial infarction treated by percutaneous transluminal coronary angioplasty in the acute phase. *J Nucl Cardiol.* 2004;11:673–681.
18. Go V, Bhatt MR, Hendel RC. The diagnostic and prognostic value of ECG-gated SPECT myocardial perfusion imaging. *J Nucl Med.* 2004;45:912–921.
19. Vanhove C, Lahoutte T, Defrise M, et al. Reproducibility of left ventricular volume and ejection fraction measurements in rat using pinhole gated SPECT. *Eur J Nucl Med Mol Imaging.* 2005;32:211–220.
20. Vanhove C, Defrise M, Franken PR, et al. Interest of the ordered subsets expectation maximization (OS–EM) algorithm in pinhole SPET reconstruction: a phantom study. *Eur J Nucl Med.* 2000;27:140–146.
21. Vanhove C, Franken PR, Defrise M, et al. Reconstruction of gated myocardial perfusion SPET incorporating temporal information during iterative reconstruction. *Eur J Nucl Med Mol Imaging.* 2002;29:465–472.

22. Germano G, Kiat H, Kavanagh PB, et al. Automatic quantification of ejection fraction from gated myocardial perfusion SPECT. *J Nucl Med.* 1995;36: 2138–2147.
23. Germano G, Kavanagh PB, Berman DS. An automatic approach to the analysis, quantitation and review of perfusion and function from myocardial perfusion SPECT images. *Int J Card Imaging.* 1997;13:337–346.
24. Cerqueira MD, Weissman NJ, Dilsizian V, et al. American Heart Association Writing Group on Myocardial Segmentation and Registration for Cardiac Imaging: standardized myocardial segmentation and nomenclature for tomographic imaging of the heart—a statement for healthcare professionals from the Cardiac Imaging Committee of the Council on Clinical Cardiology of the American Heart Association. *Circulation.* 2002;105:539–542.
25. Petzold R, Zeilhofer HF, Kalender WA. Rapid protyping technology in medicine: basics and applications. *Comput Med Imaging Graph.* 1999;23:277–284.
26. Omerovic E, Bollano E, Soussi B, et al. Selective beta1-blockade attenuates post-infarct remodelling without improvement in myocardial energy metabolism and function in rats with heart failure. *Eur J Heart Fail.* 2003;5:725–732.
27. Sjaastad I, Sejersted OM, Ilebekk A, et al. Echocardiographic criteria for detection of postinfarction congestive heart failure in rats. *J Appl Physiol.* 2000;89:1445–1454.
28. Maskali F, Poussier S, Marie PY, et al. High-resolution simultaneous imaging of SPECT, PET, and MRI tracers on histologic sections of myocardial infarction. *J Nucl Cardiol.* 2005;12:229–230.
29. Salin H, Maitrejean S, Mallet J, et al. Sensitive and quantitative co-detection of two mRNA species by double radioactive in situ hybridization. *J Histochem Cytochem.* 2000;48:1587–1592.
30. Lamaziere JM, Lavallee J, Zunino C, et al. Semiquantitative study of the distribution of two cellular antigens by computer-directed color analysis. *Lab Invest.* 1993;68:248–252.
31. Baumgartner H, Porenta G, Lau YK, et al. Assessment of myocardial viability by dobutamine echocardiography, positron emission tomography and thallium-201 SPECT: correlation with histopathology in explanted hearts. *J Am Coll Cardiol.* 1998;32:1701–1708.
32. Liu Z, Barrett HH, Stevenson GD, et al. High-resolution imaging with ^{99m}Tc-glucarate for assessing myocardial injury in rat heart models exposed to different durations of ischemia with reperfusion. *J Nucl Med.* 2004;45:1251–1259.
33. Liu Z, Kastis GA, Stevenson GD, et al. Quantitative analysis of acute myocardial infarct in rat hearts with ischemia-reperfusion using a high-resolution stationary SPECT system. *J Nucl Med.* 2002;43:933–939.
34. Nagueh SF, Mikati I, Weilbaecher D, et al. Relation of the contractile reserve of hibernating myocardium to myocardial structure in humans. *Circulation.* 1999; 100:490–496.
35. Sciagra R. Nitrates and viability: a durable affair. *J Nucl Med.* 2003;44:752–755.
36. Weisman HF, Bush DE, Mannisi JA, et al. Cellular mechanisms of myocardial infarct expansion. *Circulation.* 1988;78:186–201.